

**LINEARIZED PLANING-SURFACE THEORY  
WITH SURFACE TENSION.  
PART II: DETACHMENT WITH DISCONTINUOUS SLOPE**

E. O. TUCK

(Received 1 May 1980)

(Revised 12 November 1980)

**Abstract**

In Part I of this series, surface tension was included in the classical two-dimensional planing-surface problem, and the usual smooth-detachment trailing-edge condition enforced. However, the results exhibited a paradox, in that the classical results were not approached in the limit as the surface tension approached zero. This paradox is resolved here by abandoning the smooth-detachment condition, that is, by allowing a jump discontinuity in slope between the planing surface and the free surface at the trailing edge. A unique solution is obtainable for any input planing surface at fixed wetted length if one allows such jumps at both leading and trailing edges. If, as is the case in practice, the wetted length is allowed to vary, uniqueness may be restored by requiring either, but not both, of these slope discontinuities to vanish. The results of Part I correspond to the seemingly more-natural choice of making the trailing-edge detachment continuous, but it appears that the correct choice is to require the leading-edge attachment to be continuous.

**1. Introduction**

In Part I ([5], denoted as *I* from now on), surface tension was included in the formulation of the classical linearized planing-surface problem. This problem was then solved numerically, subject to the usual smooth-detachment condition at the trailing edge. That is, in *I* it is assumed that the slope of the free surface agrees with the slope of the planing surface at their point of contact at the rear of the planing surface. This is the usual assumption in planing-surface theory, and is analogous to the Kutta condition of aerodynamics.

The resulting solution is singular at the leading edge. This is not unexpected, and, in itself, not a cause for alarm. Indeed, the classical solution (in the absence of surface tension) already has such a singularity in the free-surface slope, which tends to infinity at the forward contact point. That is, the free surface is asymptotically vertical at this point, according to the linearized theory. If a local nonlinear analysis is performed, as was done in [7], page 587, this singularity is revealed to be a representation of spray formation at the leading edge. In fact, the leading-edge singularity in the free-surface slope is weakened by the introduction of surface tension, and the results of  $I$  show only a jump discontinuity in slope. That is, the free surface slope is now large but not infinite, just ahead of the planing surface.

Nevertheless, the results in  $I$  do not appear to be physically acceptable. In general, we must always expect capillary (short) waves ahead of the planing surface, and gravity (long) waves behind it. If the surface tension is made to vanish, the capillary wavelength goes to zero, and ultimately these waves should disappear, that is, their amplitude should tend to zero. This is not a property satisfied by the solution given in  $I$ . When computations are performed for smaller and smaller values of (scaled) surface tension, the capillary waves, far from disappearing, appear to have larger and larger amplitude. At the same time, the hydrodynamic pressure loading on the planing surface is qualitatively and quantitatively dissimilar to the classical values.

This paradox is resolved in the present work by abandonment of the smooth-detachment condition at the trailing edge. That is, we now recognise that, in the presence of surface tension, the fluid must be allowed to determine for itself at what angle its free surface departs from the planing surface. We no longer have the right to insist on that angle being zero. Analytic solutions are obtained in the long wave limit in Section 3 and numerical solutions in Section 4 for an arbitrary input planing surface.

It is interesting to note that this somewhat-surprising conclusion has also been arrived at recently by Vanden Broeck [6], in a slightly different context. Ackerberg [1] included surface tension in the classical Kirchhoff free-streamline theory for the cavity behind a flat plate. The intent of Ackerberg's analysis was to use surface tension to eliminate the infinite-curvature singularity of the classical theory at the point of contact between the free streamline and the plate, and in this respect was successful. Ackerberg's free surface joined the plate smoothly, with continuous slope and finite curvature. However, his solution was itself physically unacceptable, because it introduced a set of downstream capillary waves on the boundary of the cavity. In the absence of gravity, such waves can only be upstream of a disturbing source. A partial resolution of this difficulty was achieved by Cumberbatch and Norbury [2], who performed a

local analysis near the point of contact and verified that solutions with finite curvature, but not unacceptable waves, are possible.

The final resolution of the paradox in this cavity-flow problem was achieved by Vanden Broeck [6], who provided a complete numerical solution with no trailing waves. In order to do this, however, he had to abandon the condition of continuity of slope. That is, his solutions joined the plate with infinite curvature, but the free surface and plate made a non-zero angle at their point of contact. However, if the surface tension tended to zero, that angle also tended to zero, and the classical results were recovered.

A similar situation occurs in the present problem; however, mere relaxation of the trailing-edge detachment condition is not sufficient to yield physically-acceptable solutions. For a completely-prescribed planing-surface geometry (on a fixed wetted length), the numerical method outlined in Section 4 now determines a unique solution, possessing non-zero slope discontinuities at *both* leading and trailing edges. In general, such solutions still possess large capillary waves ahead of the body, whose amplitude grows without bound as the surface tension is reduced. However, in practice, planing does not occur at fixed wetted length. That is, we are not normally in a position to prescribe the complete geometry of the input hull *a priori*, but must allow a degree of freedom, equivalent to variation in the effective wetted length. Thus, the real planing-surface problem is one in which there is one free parameter, and the numerical method of Section 4 will then provide a one-parameter family of solutions. Among that family is one member that is physically acceptable, that is, whose capillary-wave amplitude tends to zero as the surface tension is allowed to vanish. The criterion for selecting that member appears to be that the attachment between free surface and planing surface at the *leading* edge occur without a discontinuity in slope. Solutions corresponding to enforcement of this subsidiary condition are obtained in Section 5. Although some arguments in favour of this “reversed Kutta condition” are advanced in Section 6, it remains an empirical conclusion, awaiting further research, especially of an experimental nature.

There is clearly not a great deal of relevance of the present analysis to the actual naval architectural task of designing planing boats. It is generally considered that nothing about surface tension can be important beyond scales comparable to the meniscus, that is, beyond distances of the order of a centimetre or two from the points of contact between vehicle and water surface. However, that is precisely where the interesting details of the present flow occur, and there is therefore some value in the present resolution of a difficult singular property of the solution at such contact points. In fact, the onset of actual planing is a somewhat delicate process, sensitive to small details of the flow, and it is possible that surface tension effects could be relevant to planing-boat design after all.

In addition, there are other potential or actual applications, such as to surface-living insects [3] or to industrial processes, such as skimming of impurities from surfaces of molten metal, where the surface tension is relatively of much greater importance than it is in the naval application. For these reasons, further study of this challenging problem seems warranted.

## 2. The planing integral equation

If  $\bar{\eta}(x)$  is the free-surface displacement induced on a stream of speed  $U$  and density  $\rho$  by an external pressure distribution  $\rho U^2 \bar{P}(x)$  of a general character, imposed on  $y = 0_+$ ,  $-\infty < x < \infty$ , then

$$\bar{\eta}(x) = \int_{-\infty}^{\infty} d\xi \bar{P}(\xi) K'(x - \xi), \quad (2.1)$$

where  $K'(x)$  is the displacement induced by a point pressure impulse  $\bar{P}(x) = \delta(x)$ . The function  $K'(x)$  can be expressed in terms of sine and cosine integrals ( $I$ , Equation (2.3)) and computed easily; it contains a jump discontinuity in slope of magnitude

$$K''(0_+) - K''(0_-) = \rho U^2 / T, \quad (2.2)$$

where  $T$  is the surface tension.

In  $I$ , it is established that (2.1), considered as an integral equation for an unknown  $\bar{P} = P(x)$ , given  $\bar{\eta} = \eta(x)$  on some interval  $(-l, l)$ , possesses no smooth solution  $P(x)$ . No solution exists even if we allow a general vertical displacement  $C$ , that is, if

$$\bar{\eta}(x) = \eta(x) + C, \quad (2.3)$$

with  $\eta(x)$  given, and  $C$  to be determined. However, a smooth solution does exist for a general rigid-body displacement and rotation of the input hull, that is,

$$\bar{\eta}(x) = \eta(x) + C - \alpha x, \quad (2.4)$$

where  $\eta(x)$  is given and  $C$  and  $\alpha$  are both constants to be determined. If it happens that  $\eta(x)$  is a linear function of  $x$  (that is, the input surface has a flat bottom) the only such solution is  $\bar{P}(x) \equiv 0$  and  $\bar{\eta}(x) \equiv 0$ .

The remedy to this difficulty is to allow  $\bar{P}(x)$  to be non-smooth, specifically to allow isolated pressure points. The only relevant locations for such singularities are at the leading and trailing edges  $x = \pm l$ , that is,

$$\bar{P}(x) = P_L \delta(x + l) + P_T \delta(x - l) + P(x). \quad (2.5)$$

In  $I$ , we set  $P_T = 0$ , thereby guaranteeing that there is no jump in slope at the trailing edge  $x = l$ , and then observed that unique solutions are obtainable when

$\bar{\eta}(x)$  is in the form (2.3). That is, we were able to find two unique constants  $P_L$  and  $C$  and a unique smooth function  $P(x)$ .

If both  $P_L$  and  $P_T$  may be non-zero, the integral equation is of the form

$$\bar{\eta}(x) = P_L K'(x+l) + P_T K'(x-l) + \int_{-l}^l d\xi P(\xi) K'(x-\xi). \quad (2.6)$$

As there are again two unknown constants  $P_L$  and  $P_T$ , as well as a smooth function  $P(x)$  to determine, we expect that (2.6) will possess a unique solution for any given input  $\bar{\eta}(x) \equiv \eta(x)$ . Such an expectation is confirmed in the sections to follow, both by long-wave limiting results as in  $I$ , and by computational experience.

The integral equation (2.6) is thus self-contained, in that no additional condition, equivalent to the Kutta condition of aerodynamics, is required to render the solution unique. However, in view of (2.2), any solution with both  $P_L$  and  $P_T$  non-zero, necessarily generates a free surface with a slope discontinuity at both ends  $x = \pm l$ , and hence non-smooth attachment and detachment between free surface and planing surface. The solutions in  $I$  correspond to modifications to the input, as in (2.3), to enable  $P_T = 0$ , and hence to avoid this discontinuity at the trailing edge  $x = l$ . In practice, a vertical displacement, as in (2.3), is equivalent to allowing the water to establish its own choice of wetted length.

A particular choice of importance is  $\bar{\eta}(x) \equiv 1$ , which corresponds to a flat planing surface at zero angle of attack. Solutions for this case are determined below, having  $P_L$  and  $P_T$  non-zero. We may now observe that, if  $\bar{\eta}(x)$  is given by (2.3), the general solution is

$$\left. \begin{aligned} P(x) &= P_0(x) + CP_1(x) \\ P_L &= P_L^0 + CP_L^1 \\ P_T &= P_T^0 + CP_T^1 \end{aligned} \right\}, \quad (2.7)$$

where  $\{P_0(x), P_L^0, P_T^0\}$  is the unique solution for the input  $\bar{\eta}(x) = \eta(x)$ , and  $\{P_1(x), P_L^1, P_T^1\}$  the unique solution corresponding to  $\bar{\eta}(x) \equiv 1$ .

That is, as  $C$  varies (or, equivalently, as the wetted length varies), we obtain a one-parameter family of solutions, corresponding to a vertical displacement of the original input hull. The solutions in  $I$  can be interpreted as a determination of the unique member

$$C = -P_T^1 / P_T^0, \quad (2.8)$$

of that family, such that  $P_T$  vanishes. Having set up a computational procedure in  $I$  to determine any one such member for any input  $\eta(x)$ , it is only necessary to solve, as below, for  $\bar{\eta}(x) \equiv 1$ , in order to determine *every* member of the family.

It should, however, be noted that another important special member of this family has

$$C = -P_L^1/P_L^0, \tag{2.9}$$

corresponding to  $P_L = 0$ . Although this member could be obtained as indicated above, it is obviously more convenient simply to interchange the roles of leading and trailing edges in the procedure used in  $I$ .

### 3. Long-wave limit

The kernel function  $K'$  has the small- $x$  expansion (see  $I$ ):

$$K'(x) = \frac{1}{\pi\nu} \log \frac{k_+}{k_-} + \left(\frac{k_+ - k_-}{2\nu}\right)|x| - \left(\frac{k_+ + k_-}{\nu}\right)x - \left(\frac{k_+^2 - k_-^2}{2\pi\nu}\right)x^2 \log x + O(x^2), \tag{3.1}$$

where  $k_+$  and  $k_-$  are the capillary and gravity wave numbers, and  $\nu$  is a constant.

If  $k_+l$  and  $k_-l$  are both small, that is, if the length of the planing surface is small compared to the wavelength of both sets of waves, then  $K'$  can be approximated by (3.1) in the integral equation (2.6). That is,

$$\begin{aligned} \eta(x) = & P_L \left[ \frac{1}{\pi\nu} \log \frac{k_+}{k_-} - \frac{k_+ + 3k_-}{2\nu}(x + l) - \frac{k_+^2 - k_-^2}{2\pi\nu}(x + l)^2 \log(x + l) \right] \\ & + P_T \left[ \frac{1}{\pi\nu} \log \frac{k_+}{k_-} - \frac{3k_+ + k_-}{2\nu}(x - l) - \frac{k_+^2 - k_-^2}{2\pi\nu}(x - l)^2 \log(l - x) \right] \\ & + \int_{-l}^l \left( \frac{1}{\pi\nu} \log \frac{k_+}{k_-} + \frac{k_+ + k_-}{\nu} \xi \right) P(\xi) d\xi - \left( \frac{k_+ + k_-}{\nu} \right) x \int_{-l}^l P(\xi) d\xi \\ & + \left( \frac{k_+ - k_-}{2\nu} \right) \int_{-l}^l P(\xi) |x - \xi| d\xi. \end{aligned} \tag{3.2}$$

Two differentiations of (3.2) indicate that

$$\begin{aligned} \eta''(x) = & -((k_+^2 - k_-^2)/\pi\nu)[P_L \log(x + l) + P_T \log(l - x)] \\ & + ((k_+ - k_-)/\nu)P(x). \end{aligned} \tag{3.3}$$

We now assume that

$$\eta(x) = C - \alpha x, \tag{3.4}$$

for suitable constants  $C$  and  $\alpha$ , so that  $\eta'' = 0$ , and hence

$$P(x) = ((k_+ + k_-)/\pi)[P_L \log(x + l) + P_T \log(l - x)]. \tag{3.5}$$

Equation (3.5) has a leading-order error equivalent to replacing each of the logarithms by a constant.

Now if we return to the undifferentiated equation (3.2), it is clear from (3.5) that the terms in  $P(x)$  can be neglected, to leading order. That is, keeping only leading-order coefficients of the linear terms,  $P_L$  and  $P_T$  are determined from

$$C = (P_L + P_T) \left( \frac{1}{\pi\nu} \log \frac{k_+}{k_-} \right), \quad (3.6)$$

and

$$\alpha = P_L \left( \frac{k_+ + 3k_-}{2\nu} \right) + P_T \left( \frac{3k_+ + k_-}{2\nu} \right), \quad (3.7)$$

the solution of which is

$$P_L = -\frac{\alpha\nu}{k_+ - k_-} + \frac{C\pi\nu(3k_+ + k_-)}{2(k_+ - k_-) \log(k_+/k_-)}, \quad (3.8)$$

and

$$P_T = \frac{\alpha\nu}{k_+ - k_-} - \frac{C\pi\nu(k_+ + 3k_-)}{2(k_+ - k_-) \log(k_+/k_-)}. \quad (3.9)$$

This completes the demonstration that a complete solution can be obtained in this long-wave limit, at least for flat planing surface given by (3.4). If  $\eta''(x) \cong 0$ ,  $P(x)$  contains  $O(1)$  terms that directly influence the determination of  $P_L$  and  $P_T$ , but these quantities can still be determined without difficulty.

The relationships (3.6), (3.7), or, equivalently, (3.8), (3.9), can be considered as two equations connecting four quantities  $C$ ,  $\alpha$ ,  $P_L$  and  $P_T$ . It is not really important which two of these we consider unknown, and which we consider known. For example, if both  $P_L$  and  $P_T$  are zero, clearly  $C = 0$  and  $\alpha = 0$  also. This trivial solution corresponds to a rigid-body rotation of the input hull, until it does not disturb the flow. If  $C = 1$  and  $\alpha = 0$ , we obtain results relevant to the solution to be presented in the following section; note that  $P_L > 0$ ,  $P_T < 0$ , and  $P_L + P_T > 0$  in such a case.

If either  $P_L$  or  $P_T$  is made to vanish,  $C$  may be considered as an unknown. The case  $P_T = 0$  was solved in *I*. In the present article, we are also interested in  $P_L = 0$ , in which case

$$C = \frac{2\alpha}{\pi} \left[ \frac{\log(k_+/k_-)}{3k_+ + k_-} \right], \quad (3.10)$$

and

$$P_T = \frac{2\nu\alpha}{3k_+ + k_-}. \quad (3.11)$$

The result (3.5) shows that  $|P(x)| \rightarrow \infty$  as  $x \rightarrow \pm l$ , whenever  $P_L \neq 0$  and  $P_T \neq 0$ . In particular, if  $P_T > 0$ , (as, for example, is indicated by (3.11)), then

$$P(x) \sim \log(l - x) \rightarrow -\infty \quad \text{as } x \rightarrow l. \tag{3.12}$$

That is, a weak negative infinity in the disturbed pressure  $P(x)$  is expected near the trailing edge, if the trailing-edge impulse  $P_T$  is positive. On the other hand, (3.5) gives us no information about the behaviour of  $P(x)$  near an end where the strength of the impulse is zero. However, the derivation of (3.5) suggests that, if (say)  $P_L = 0$ , then  $P(x)$  will remain bounded as  $x \rightarrow -l_+$ , and computational experience confirms this.

Although the above results are formally true only in the long-wave limit  $k_{\pm}l \rightarrow 0$ , the qualitative features indicated should also be true for arbitrary  $k_{\pm}l$ .

#### 4. Solution for given $\bar{\eta}(x)$

Our task is to solve the integral equation (2.6) for  $P(x)$ , given the function  $\bar{\eta}(x)$  on  $(-l, l)$ . Assuming, as in  $I$ , that  $P(x) = P_j = \text{constant}$  on the  $j$ th of a set of  $N$  intervals  $(x_{j-1}, x_j)$  into which  $(-l, l)$  is divided, we have

$$\bar{\eta}(x) = P_L K'(x + l) + P_T K'(x - l) + \sum_{j=1}^N P_j [K(x - x_{j-1}) - K(x - x_j)]. \tag{4.1}$$

Equation (4.1) contains  $N + 2$  unknowns  $P_L, P_T, P_1, P_2, \dots, P_N$  and we need  $N + 2$  equations, obtained by forcing (4.1) to hold at  $N + 2$  values of  $x$ .

A convenient set of such values is that consisting of the  $N$  mid-points

$$\bar{x}_i = (x_{i-1} + x_i)/2 \tag{4.2}$$

and the two ends of the range,  $\bar{x}_0 = -l$  and  $\bar{x}_{N+1} = +l$ . If, at the same time, we denote  $P_0 = P_L$  and  $P_{N+1} = P_T$ , the resulting set of equations can be displayed in terms of a vector of unknowns

$$\mathbf{p} = [P_j] \quad \text{for } j = 0, 1, 2, \dots, N, N + 1, \tag{4.3}$$

and an input vector

$$\mathbf{b} = [\bar{\eta}(\bar{x}_i)] \quad \text{for } i = 0, 1, 2, \dots, N, N + 1, \tag{4.4}$$

as

$$\mathbf{A}\mathbf{p} = \mathbf{b}, \tag{4.5}$$

where, for all  $i = 0, 1, 2, \dots, N, N + 1$ , the matrix  $A$  has components

$$\left. \begin{aligned} A_{i0} &= K'(\bar{x}_i + l), \\ A_{i,N+1} &= K'(\bar{x}_i - l) \quad \text{and} \\ A_{ij} &= K(\bar{x}_i - x_{j-1}) - K(\bar{x}_i - x_j) \quad \text{for } j = 1, 2, \dots, N. \end{aligned} \right\} \quad (4.6)$$

The above discretization is similar to that used in  $I$ . However, in that case a preliminary differentiation enabled elimination of one of the unknowns, and the equation was then forced to hold at end-points, rather than mid-points of intervals. However, there appears to be no difference in the rates of convergence in these two cases. Since both  $K$  and  $K'$  are continuous functions, no difficulty occurs in the evaluation of all matrix elements by (4.6).

The matrix  $A$  may be inverted without difficulty, and yields results with about 3-figure accuracy at  $N = 50$ , except for values of surface tension so low that the capillary wavelength  $2\pi/k_+$  is comparable to the mean mesh size  $2l/N$ , and even then yields at least two figures. A typical check on accuracy (at  $\bar{\eta}(x) \equiv 1$ ) is obtained by re-computing  $\bar{\eta}(x)$  directly from (4.1), once  $\mathbf{p}$  has been determined. Of course, (4.1) will be satisfied *exactly* when  $x = \bar{x}_i$ . However, if we allow  $x$  to take values other than  $\bar{x}_i$ , the computed values differ from unity only in the third decimal place at  $N = 50$ .

In a certain sense, every inversion of  $A$  yields an exact solution. That is, the expression (4.1) is not an approximation, but rather the *exact* free surface generated by a certain specific  $N$ -step pressure distribution and two given  $\delta$ -functions. We have chosen this set of numbers  $\mathbf{p}$  so that  $\bar{\eta}(x)$  agrees at a specified set of  $N + 2$  values of  $x$  with an input hull shape. We have no necessary right to expect it to agree with that shape at any other value of  $x$ , but would be unhappy with this numerical procedure if it did not. Nor do we have any necessary right to expect the results to converge as  $N \rightarrow \infty$ , but they do, with an error that tends to zero like  $N^{-2}$ .

Results are presented here only for  $\bar{\eta}(x) \equiv 1$ , and only for  $\gamma = 1$ , where

$$\gamma = gl/U^2. \tag{4.7}$$

As indicated in Section 2, in combination with the already-determined solutions of  $I$ , it is necessary only to solve the present problem for  $\bar{\eta}(x) \equiv 1$  in order to determine a whole family of solutions. However, in principle there is no reason why the present programme could not be used for any input  $\bar{\eta}(x)$ .

The results are determined as functions of the non-dimensional surface-tension parameter

$$\mu = 4gT/(\rho U^4). \tag{4.8}$$

Primary outputs are  $P_L, P_T$ , and the net lift

$$F = \int_{-l}^l P(x) dx. \tag{4.9}$$

Typical convergence is indicated by values of  $F$  at  $\mu = 0.2$  of 2.236, 2.493, 2.540, 2.556 and 2.564 for  $N = 10, 20, 30, 40$  and  $50$  respectively. This is quite a low value of surface tension, and the capillary wavelength is about 0.15 of the planing surface length  $2l$ . A 10% error at  $N = 10$  is thus already quite good, and the results at  $N = 50$  are close to 3-figure accuracy.

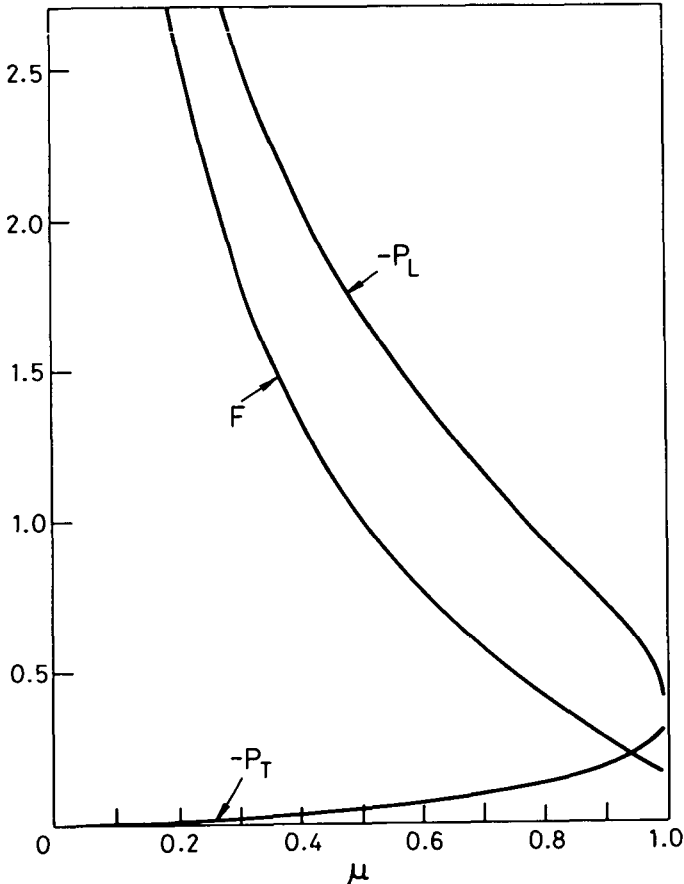


Figure 1. Leading-edge ( $P_L$ ) and trailing-edge ( $P_T$ )  $\delta$ -function strengths, and net lift coefficient ( $F$ ), plotted against scaled surface tension  $\mu$ , at  $\gamma = g/U^2 = 1$ , for  $\eta(x) = 1$ .

Figure 1 shows plots of  $P_L$ ,  $P_T$  and  $F$  against  $\mu$  at  $\gamma = 1$ . The quantities  $P_L$  and  $P_T$  are always negative. This means that the local free surface level drops below that at the point of contact. Since the input hull  $\bar{\eta} = 1$  lies above the mean surface level, such a result should be expected intuitively. The absolute

value of  $P_L$  is greater than that of  $P_T$  and, in fact, as  $\mu \rightarrow 0$ ,  $-P_T \rightarrow 0$ , while  $-P_L \rightarrow \infty$ . That is, for vanishingly small surface tension, the free surface departs tangentially from the trailing edge. Note that no condition of Kutta type has been imposed here; it is surface tension itself that provides this fore-aft asymmetry in the problem.

The behaviour of these results at the other end  $\mu \rightarrow 1$  of the range is not yet fully explained. No wave-like solution is possible for  $\mu > 1$ , and some kind of singularity would be expected as  $\mu \rightarrow 1$ . Although computational accuracy cannot be maintained right up to this limit, it does appear as if  $F$  and  $P_L$  are tending to finite values, but with rapid rates of change near  $\mu = 1$ .

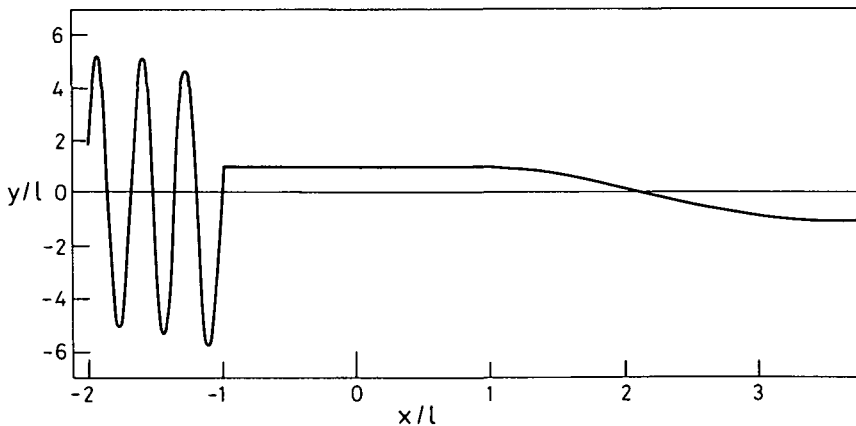


Figure 2. Example of free surface shape for  $\eta(x) = 1$ , computed at  $\mu = 0.2$  and  $\gamma = 1$ .

Figure 2 shows the free-surface shape at  $\mu = 0.2$ , computed using  $N = 50$ . The value  $P_T = -0.009$  of the trailing-edge singularity is so small that the free surface appears to leave tangentially, then developing a trailing gravity wave of approximately unit amplitude and length approximately  $2\pi$ , too long to be seen on this Figure. On the other hand, ahead of the plate there is a large short capillary wave, of amplitude about 5, which attaches at the leading edge almost vertically, since  $P_L = -3.36$  is quite large. Everywhere between leading and trailing edge, the input hull  $\bar{\eta} \equiv 1$  is reproduced to 3-figure accuracy.

The solution so obtained, possessing a large capillary wave, is no more acceptable physically than those in *I*. However, what is now clear is that if we take a solution with  $P_T = 0$  as in Figure 4 of *I*, and add a suitable multiple of the present solution, a flow with a small capillary wave can result. An important aspect of this approach is the quite small values of  $P_T$  in the present results, indicating that the resulting combination of the two solutions will still have a small  $P_T$  value, and hence nearly-tangential trailing-edge detachment.

When this process is carried out, it immediately becomes apparent that the particular choice of the vertical-shift constant  $C$  in (2.3) and (2.7) that cancels the large capillary wave ahead of the body also reduces dramatically the size of the leading-edge singularity  $P_L$ . There is no doubt from the present results, and those of  $I$ , that the large capillary waves are closely correlated with large values of  $P_L$ , and whatever linear combination reduces one, reduces the other. In particular, it is always possible to choose  $C$  as in (2.9) so as to eliminate  $P_L$  *entirely*, and we now see that this choice also almost eliminates the capillary waves. It is therefore appropriate to investigate this family of solutions further, by direct numerical methods.

### 5. Solution with $P_L = 0$

Although in principle we can solve all problems with  $P_L = 0$  by linear combinations as in (2.7), it is much more convenient to build the assumption  $P_L = 0$  directly into the numerical methods. That is, we need merely interchange the roles of leading and trailing edges in the numerical procedure outlined in  $I$ , the same computer programme being used with very minor changes. The results to be presented below have been checked with those obtained by use of (2.7), and are in good agreement. These results are all for a flat plate  $\bar{\eta}(x) = -\alpha x$ , the angle of attack  $\alpha$  being scaled to unity without loss of generality.

Figure 3 shows  $P_T$  and the net lift  $F$ , as functions of  $\mu$ , at  $\gamma = 1$ . The limiting behaviour as the surface tension  $\mu \rightarrow 0$  is now completely acceptable physically,  $P_T$  tending rapidly to zero and  $F$  linearly to the known value ( $\sim 1.09$  at  $\gamma = 1$ ) in the absence of surface tension. It is important to note that although one cannot expect good accuracy from the present programme when the capillary wavelength becomes comparable to  $2l/N$  (that is, for  $\mu < 0.02$ , if  $N$  is limited to a maximum of 50), the smooth approach to the  $\mu = 0$  limit is well established at much larger  $\mu$  values, where no doubt exists about the ability of the discretization to cope with the capillary waves.

Accuracy is also lost at the other extreme  $\mu \rightarrow 1$ . The present results appear to suggest  $F \rightarrow 0$  as  $\mu \rightarrow 1$ , while  $P_T$  is increasing rapidly very close to  $\mu = 1$  and may be tending to infinity. The neighbourhood of the critical value  $\mu = 1$  is well known to be a difficult one to study and further clarification of solution properties in this region is left for future work.

Convergence of the smooth pressure distribution  $P(x)$  is illustrated by Figure 4, in which the known pressure distribution at zero surface tension is shown dashed, to be compared with the present computations at  $\mu = 0.2, 0.5$  and  $0.8$ .

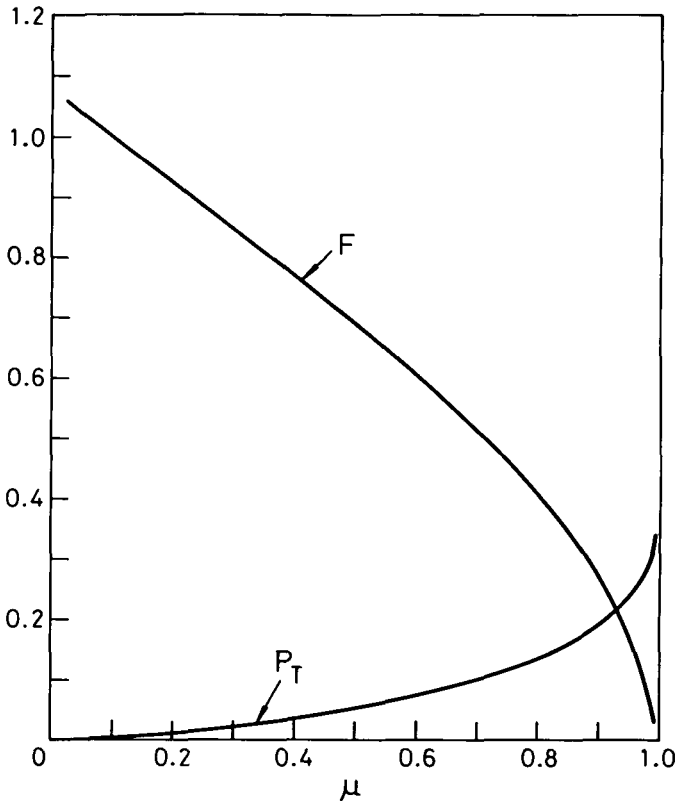


Figure 3. Trailing-edge  $\delta$ -function strength ( $P_T$ ), and net lift coefficient ( $F$ ), for a flat plate  $\eta(x) = -\alpha x + C$ , where  $\alpha$  is scaled to unity and  $C$  is determined by the programme so that the leading-edge  $\delta$ -function strength ( $P_L$ ) vanishes. Plot against  $\mu$  at fixed  $\gamma = 1$ .

The results at  $\mu = 0.2$  are clearly already quite close to the  $\mu = 0$  limit, for most  $x \neq \pm l$ . This is in contrast to the results of *I*, where the two pressure distributions were not even qualitatively alike.

The different (*indeed*, opposite!) behaviour of the pressure distributions near the ends for  $\mu = 0$  and  $\mu > 0$ , is well illustrated by this figure. Thus, in the absence of surface tension,  $P(x) \rightarrow +\infty$  as  $x \rightarrow -l$ , giving the usual leading-edge inverse-square-root singularity. However, for non-zero surface tension,  $P(x)$  appears to approach a *finite* limiting value as  $x \rightarrow -l$ , albeit with infinite slope. This is in accord with the predictions of Section 3. Conversely, although  $P(x) \rightarrow 0$  as  $x \rightarrow +l$  in the absence of surface tension, so satisfying a Kutta-type condition at the trailing edge, for non-zero surface tension,  $P(x) \rightarrow -\infty$  (logarithmically) as  $x \rightarrow +l$ , again in accord with Section 3. The fact that  $P_L = 0$ ,

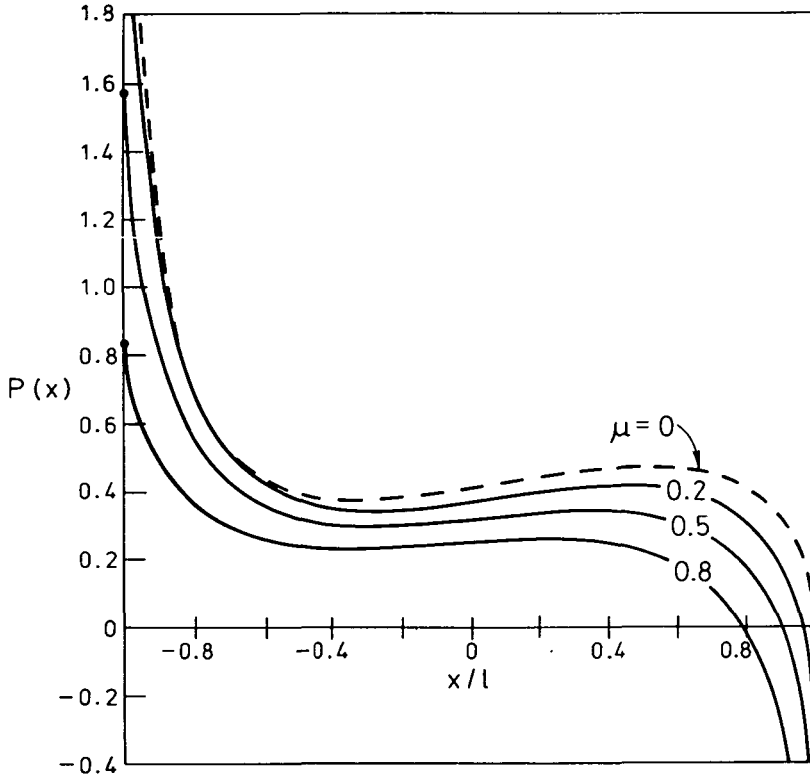


Figure 4. Pressure distribution in  $-l < x < l$  on a flat plate as in Figure 3, for various values of  $\mu$ .

but  $P_T \neq 0$ , in these computations indicates that smooth attachment occurs at the leading edge, but that the free surface detaches with discontinuous slope at the trailing edge.

Figure 5 illustrates the leading-edge attachment near  $x = -l$ . Again the dashed curve is the known result at zero surface tension, in which the attachment is non-smooth. In fact the  $\mu = 0$  free surface becomes exactly vertical (in this linearized theory) at the point of attachment, its slope tending to  $+\infty$ . In contrast, computed results shown in Figure 5 with  $\mu = 0.1$  and  $0.2$  correspond to attachment with continuous slope, that is, to a slope value of  $-\alpha$  at attachment. Since the vertical-shift parameter  $C$  in (2.3) varies as  $\mu$  varies, the three curves shown in Figure 5 correspond to slightly different vertical locations of the flat plate  $y = -\alpha x + C$ ,  $x > -l$ .

As  $\mu \rightarrow 0$ , the region near to attachment at  $x = -l$  in which the free-surface slope changes from a large positive value to the plate's value  $-\alpha$  contracts to the

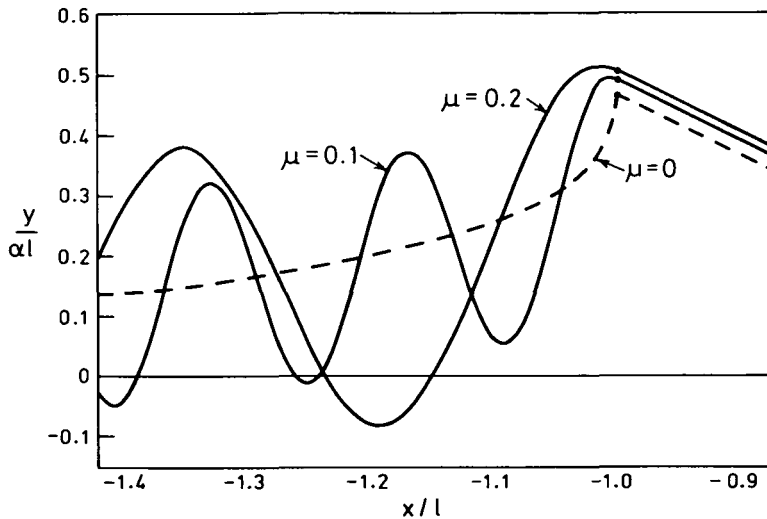


Figure 5. Expanded view of free surface near leading edge of flat plate as in Figure 3, for various values of  $\mu$ . Note that, because the value of  $C$  varies with  $\mu$ , so does the height of the plate,  $x > -l$ .

point  $x = -l$  itself. For very small  $\mu$ , except in the immediate neighbourhood of  $x = -l$ , the appearance is as if the attachment were vertical. At the same time, as  $\mu \rightarrow 0$ , the capillary waves are reducing in amplitude, although not at a very rapid rate. A similar plot to Figure 5 could be presented for the immediate neighbourhood of the *trailing* edge  $x = +l$ . This would display the fact that the free surface departs tangentially for  $\mu = 0$ , but at a finite angle for all  $\mu > 0$ . However, this angle, being proportional to  $P_T$  in Figure 3, is quite small for all  $\mu$ , and, in view of the fact that the gravity waves behind the body are not apparent close to detachment, such a plot consists simply of a set of straight lines, and is not shown here.

The above results are all for  $\gamma = 1$ . Figure 6 shows a set of computations of the lift force  $F$  as a function of  $\gamma$ , for values of  $\mu = 0, 0.2, 0.4, 0.6$  and  $0.8$ . The  $\mu = 0$  curve (dashed) is computed as by Oertel [4]. Because  $\rho, U, L$  and  $\alpha$  are all scaled to unity in this computation, the quantity  $F$  is actually the lift coefficient  $F = (\text{dimensional lift})/(\rho U^2 l \alpha)$  which tends to  $\pi$  as  $\gamma \rightarrow 0$ , when  $\mu = 0$ . The parameter  $\gamma$  measures speed inversely, the conventional wetted-length-based Froude number being  $(2\gamma)^{1/2}$ . Thus the left part of Figure 6 corresponds to high speed, the right to low speed. Oertel's [4] computations indicate that true planing (dynamic lift  $>$  buoyancy) corresponds approximately to  $\gamma < 1$ , this being the important range in practice.

Clearly surface tension is bad for lift generation, the curves with  $\mu > 0$  being uniformly lower than that for  $\mu = 0$ . In particular, at any value of  $\mu > 0$  the lift

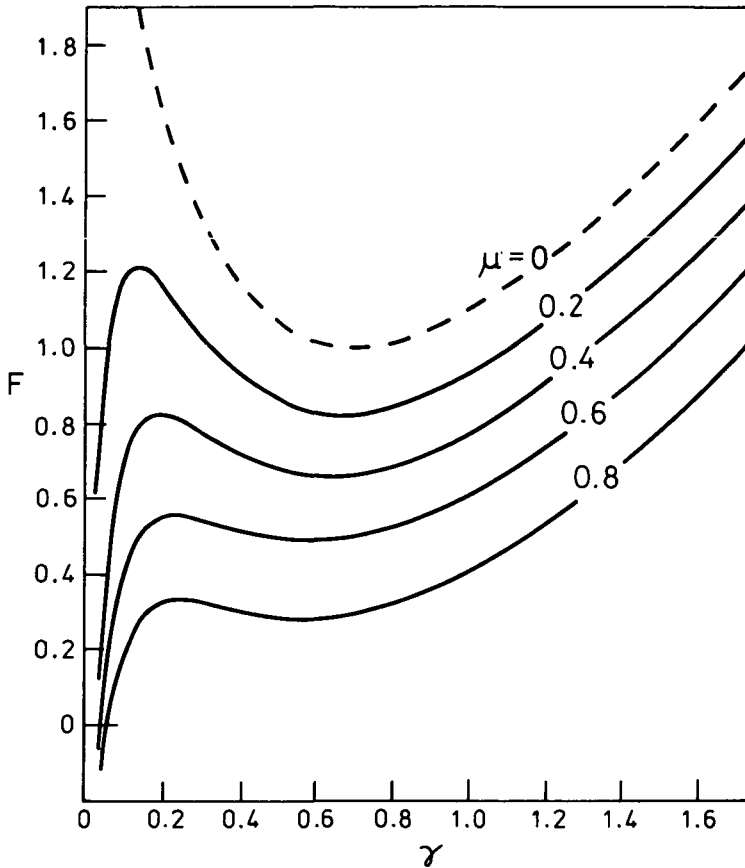


Figure 6. Lift coefficient ( $F$ ) as a function of  $\gamma = gl/U^2$ , for various values of  $\mu = 4gT/U^4$ .

coefficient peaks at a low value of  $\gamma$ , and then tends to  $-\infty$  as  $\gamma \rightarrow 0$ . This result is in accord with the long-wave asymptote derived in Section 3, which corresponds to the limit as  $\gamma \rightarrow 0$  with  $\mu$  held fixed. Care should be exercised, however, in interpreting Figure 6 as a plot of lift coefficient against (inverse) speed, since (at fixed values of the true surface tension  $T$ ) the non-dimensional parameter  $\mu$  also depends (inversely) on speed  $U$ . That is, at fixed  $T$ ,  $\rho$ ,  $g$  and wetted length  $2l$ , as we let  $\gamma \rightarrow 0$  to achieve high speed, we should also let  $\mu \rightarrow 0$ . Even this approach has its defect, however, as a model of the true planing-boat lift as a function of speed, since in practice the wetted length  $2l$  also varies with speed.

Further consideration of practical aspects of this design question, as in Oertel [4], are beyond the scope of the present paper. Other quantities of importance in

such considerations (such as the depth of the trailing edge, and the location of the centre of pressure) seem to vary rather less with  $\mu$  than does the net lift  $F$ .

## 6. Conclusion

The results of Section 5 appear to have acceptable properties, especially as  $\mu \rightarrow 0$ . It therefore appears that the correct end condition is a “reversed Kutta condition”, in which tangential attachment is enforced at the leading but not at the trailing edge.

It is, however, important to emphasize that, with surface tension, a unique solution exists for a *completely prescribed* planing surface geometry, in which hydrodynamic forces must be allowed to determine a non-zero angle of detachment at *both* ends. Even though this solution in general possesses large capillary waves ahead of the planing surface, it is undoubtedly correct wherever there is no freedom at all to adjust any parameters of the input hull. If the planing surface is of very short wetted length, and is cut off sharply at both front and back, there is no escape from such a solution. It is possible that surface-skimming insects (see [3]) induce such a flow, although it is hardly likely that nature would allow an inefficient mode with large precursor capillary waves to be used routinely for locomotion.

The situation of somewhat greater interest is that in which, although the trailing edge is perhaps sharply cut off (as in a transom stern of a conventional planing boat), there is freedom to adjust the location of the leading edge. This can occur [4] by adjustments of load distribution, *via* the angle of attack  $\alpha$ , for a fixed net load, balanced by the lift force. In that case it is not unreasonable to expect that the attachment point will adjust itself, until attachment occurs tangentially.

One can, for example, envisage a sequence of experiments being performed as sketched in Figure 7. A trapezoidal body (that is, a cut-off wedge) is submerged quite deeply. In fact, deeply enough for its whole sloping face to be wetted, but not quite so deeply as to cause water to build up onto the vertical forward face. At this maximum depth, the flow will be like the negative of that of Section 4, with a large capillary wave, and with the free surface rising at a non-zero angle from both corners.

Suppose now we raise this body slowly, holding the angle of attack of its sloping face fixed. At first, surface tension will keep the free surface attached at both corners, but the amplitude of both sets of waves will decrease, and so will the angle between the free surface and the body at the two corners. Eventually, a height will be reached at which the free surface slope at the leading edge is the

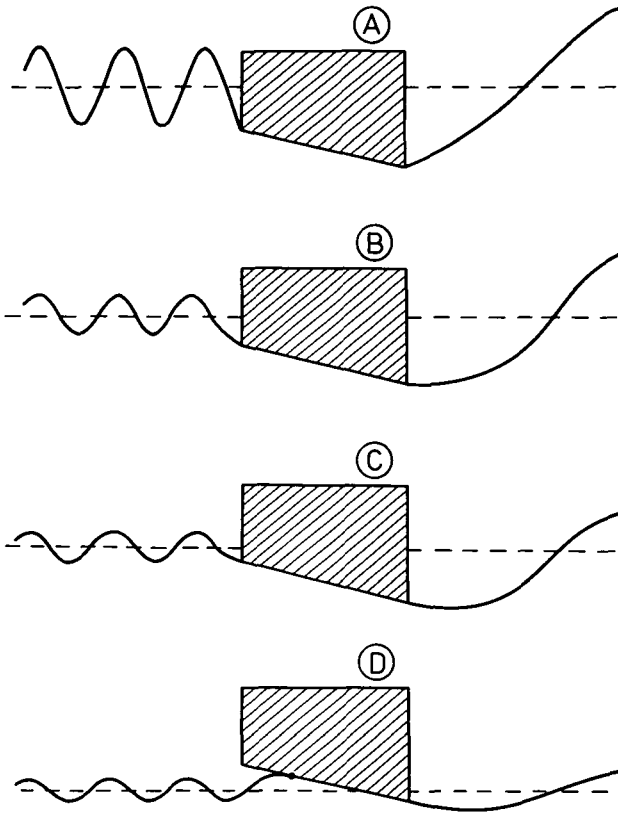


*Figure 7.* Conceptual experiment in which a wedge-like body is slowly raised in a stream of water: A: Initial deeply-submerged position, leading-edge free surface nearly vertical. B: Less deep, contact angle at leading corner reduced. C: Contact now tangential. D: Contact point moves along sloping face, remaining tangential.

same as that of the sloping face of the body. This will occur at the leading edge before it does at the trailing edge, simply because the former is higher.

If the body is now raised even further, two things could happen. Attachment could still occur at the corner, in which case a flow like that of Section 4 will be maintained. However, what is surely more plausible is that the attachment point will move aft of the forward corner. That is, the wetted length will decrease. Since this process commences with tangential attachment, there is no reason to suppose that tangential attachment will ever fail to occur. That is, at all subsequent heights, the free surface joins the sloping face at a point between the two corners, that point being determined hydrodynamically by the condition that attachment be tangential.

Until a sufficiently careful set of experiments of this nature is done, the above argument must remain speculative. However, with the support of the parallel research on cavities discussed in the Introduction, and the fact that it leads to the correct limit as  $\mu \rightarrow 0$ , the reversed Kutta condition appears to be appropriate for planing surface flows in the presence of surface tension.

### Acknowledgement

I have been worrying myself and my friends about this problem for more than four years. Among many who have lent a sympathetic ear and/or provided helpful suggestions are J. N. Newman, T. Y. Wu, D. H. Peregrine, E. Cumberbatch, L. W. Schwartz and (especially) J.-M. Vanden Broeck.

### References

- [1] R. C. Ackerberg, "The effects of capillarity on free-streamline separation", *J. Fluid Mech.* 70 (1975), 333–352.
- [2] E. Cumberbatch and J. Norbury, "Capillary modification of the singularity at a free-streamline separation point", *Quart. J. Mech. Appl. Math.* 32 (1979), 303–312.
- [3] L. J. Milne and M. Milne, "Insects of the water surface", *Scientific American* (April 1978), 134–142.
- [4] R. P. Oertel, *The steady motion of a flat ship including an investigation of local flow near the bow* (Ph.D. Thesis, University of Adelaide, 1974).
- [5] E. O. Tuck, "Linearized planing-surface theory with surface tension. Part I: Smooth detachment", *J. Austral. Math. Soc. Ser. B* (1982), 241–258.
- [6] J.-M. Vanden Broeck, "The influence of capillarity on cavitating flow past a flat plate", *Quart. J. Mech. Appl. Math.* 34 (1981), (in press).
- [7] J. V. Wehausen and E. V. Laitone, "Surface waves", in *Handb. der Physik*, Vol. 9, ed. S. Flugge (Springer-Verlag, Berlin, 1960).

Department of Applied Mathematics  
University of Adelaide  
Box 498, G.P.O.  
Adelaide  
South Australia 5001